

Supporting Information

Manganese Self-boosting Hollow Nanoenzymes with Glutathione Depletion for Synergistic Cancer Chemo-chemodynamic Therapy

Xinyi Cai^{1,‡}, Deng Cai^{2,‡}, Xiaozhen Wang^{3,‡}, Dou Zhang¹, Long Qiu¹, Zhenying Diao¹, Yong Liu¹, Jianbo Sun¹, Daxiang Cui^{4,*}, Yanlei Liu^{5,*}, Ting Yin^{1,*}

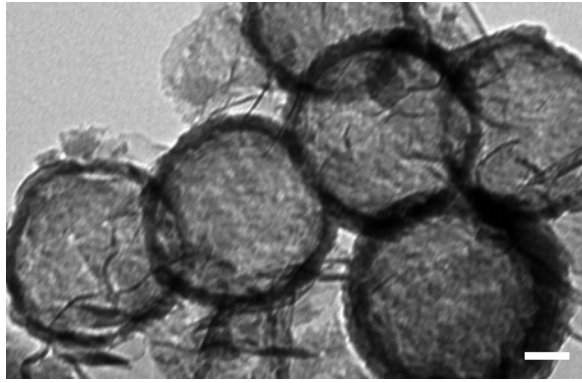


Figure S1. TEM image of HMnO₂. Scale bar: 50 nm

Table S1. Drug content in HMnO₂@CDDP determined by ICP.

CDDP used for synthesis [mg]	Remaining CDDP content after synthesis [mg]	CDDP loading efficiency [%]	Average loading efficiency [%]
5	1.91	61.80%	62.70%
	1.83	63.40%	
	1.85	63.00%	

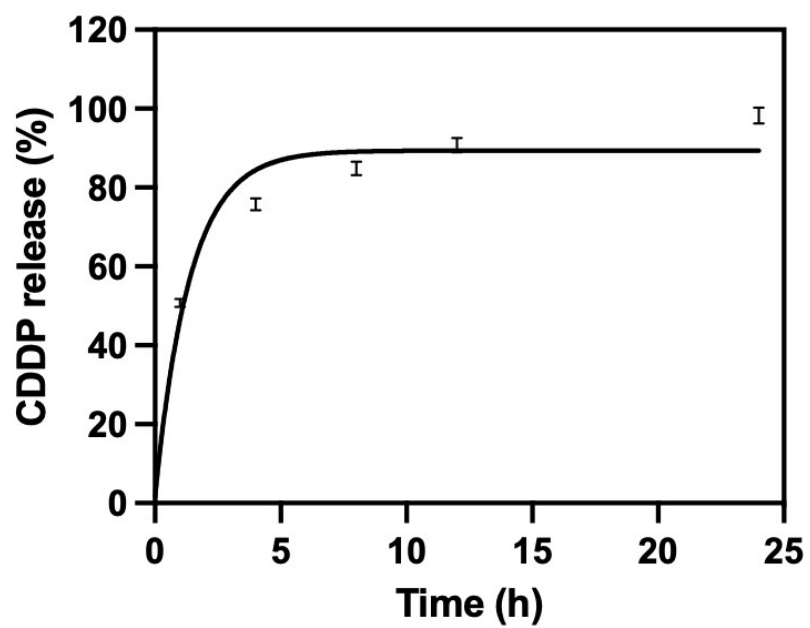


Figure S2. CDDP release profiles of HMnO₂@CDDP at different time points.

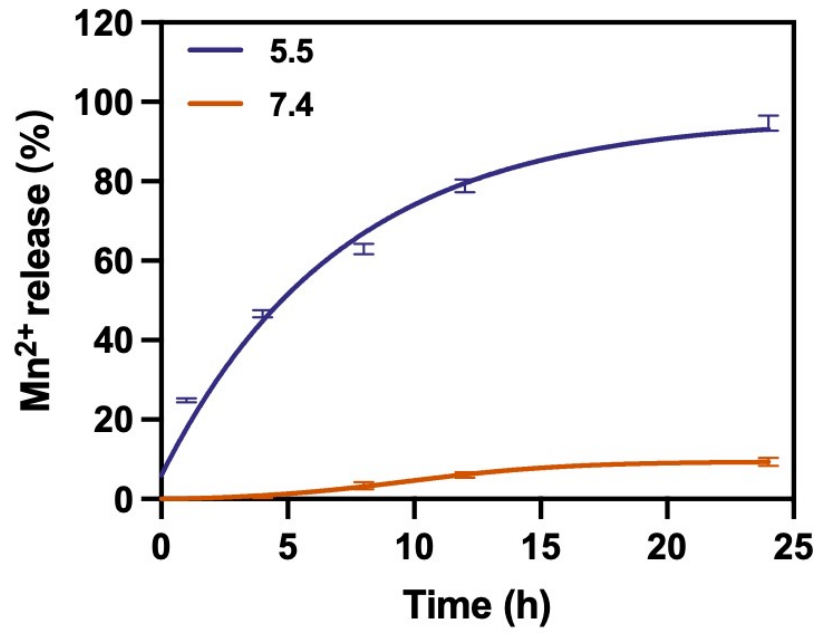


Figure S3. Mn²⁺ release profiles of HMnO₂@CDDP at different pH values.

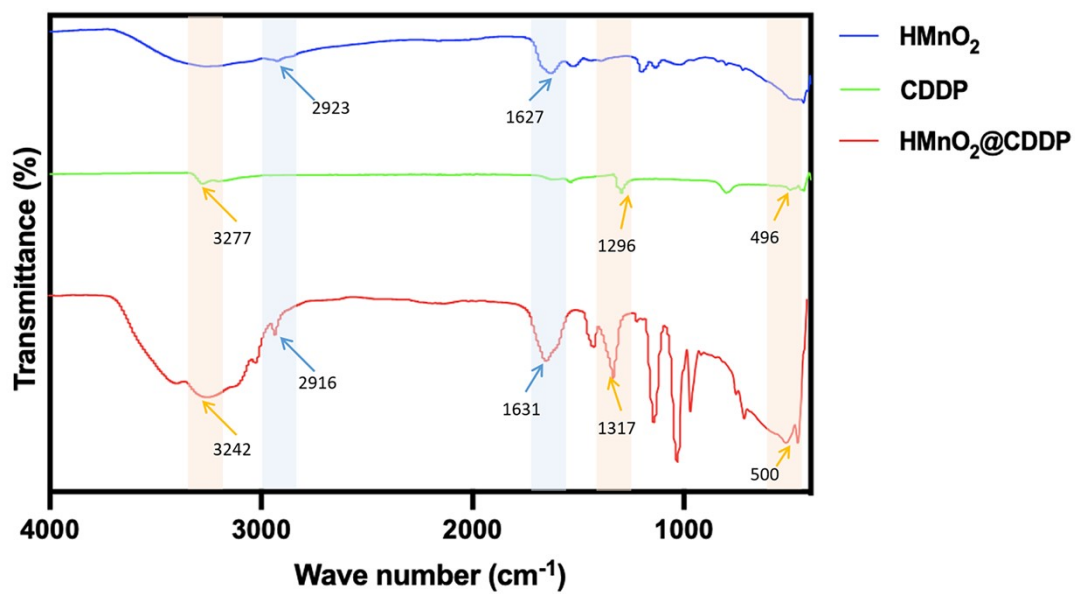


Figure S4. FTIR spectra of HMnO_2 , CDDP and $\text{HMnO}_2@\text{CDDP}$.

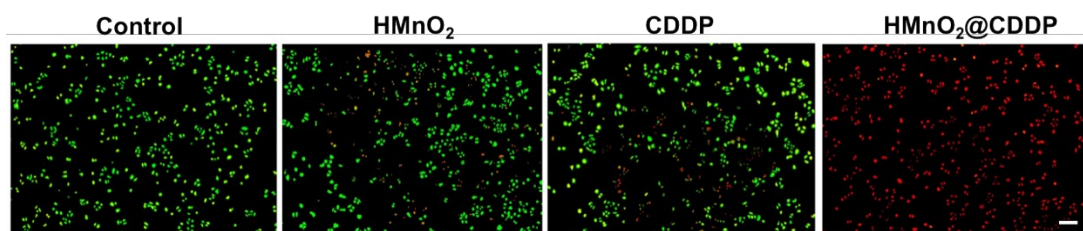


Figure S5. Fluorescence images of Calcein AM (green, live cells) and PI (red, dead cells) co-stained A549 cells treated by different formulations. Scale bar: 100 μ m.

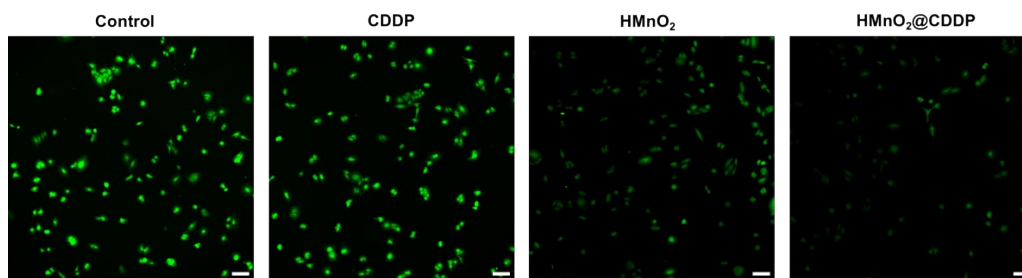


Figure S6. Fluorescence images of intracellular GSH in A549 cells after treated by different formulations for 12 h. Scale bar: 100 μm.

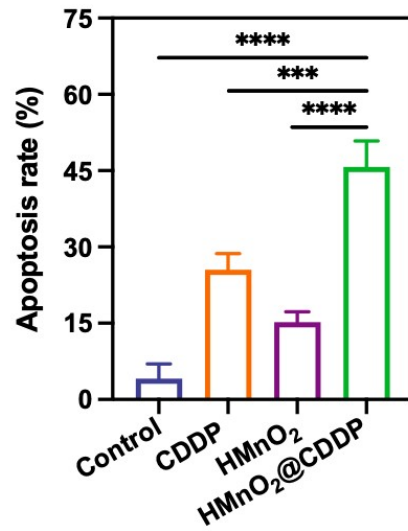


Figure S7. Quantitative analyses of apoptosis in A549 cells treated by different formulations for 12 h. The results are represented as mean \pm standard deviation (n = 3 per group).

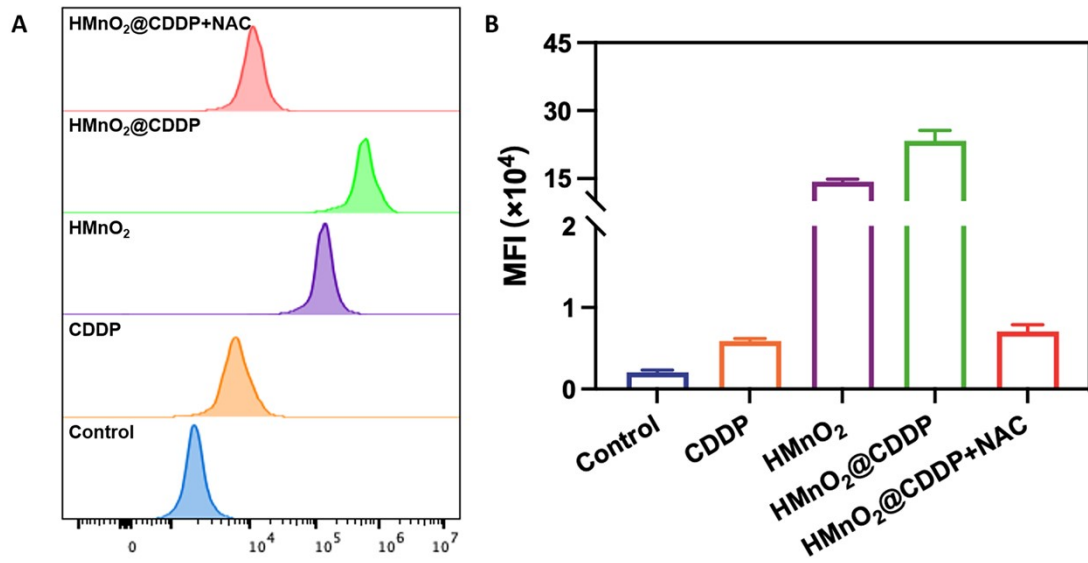


Figure S8. Flow cytometric and quantitative analyses of intracellular $\cdot\text{OH}$ level for A549 cells after being treated by different formulations for 12 h.

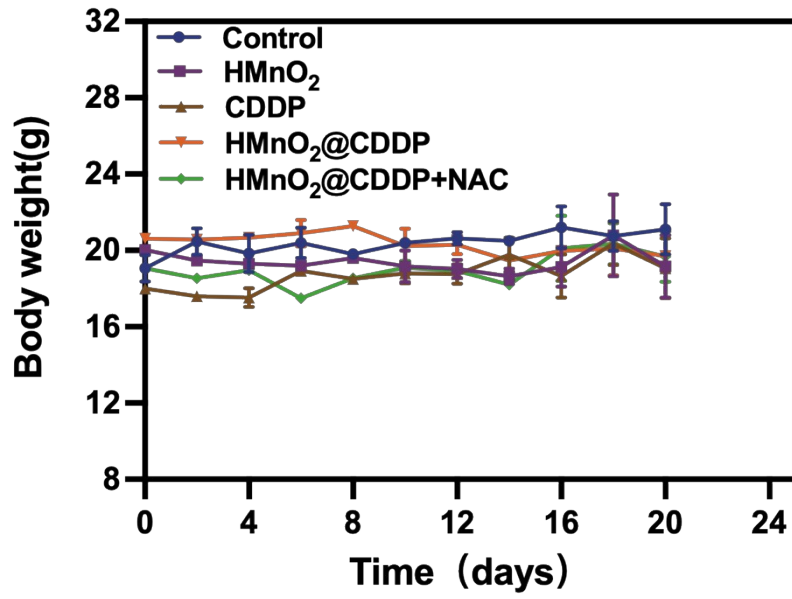


Figure S9. Body weight changes of mice with different treatments.